

The Heavy Nuclei of the Primary Cosmic Radiation*

P. S. FREIER, G. W. ANDERSON, J. E. NAUGLE, AND E. P. NEY

University of Minnesota, Minneapolis, Minnesota

(Received May 31, 1951)

The atmospheric absorption of the flux of nuclei of charge ≥ 10 has been obtained at $\lambda = 55^\circ$ N from a combination of flux measurements at different altitudes and at different zenith angles. The absorption, together with the collision cross section, gives an energy spectrum consistent with the one measured by stopping particles and the latitude effect. The cross section for collision of heavy nuclei is about three-fourths of the geometric cross section. The energy spectrum can be represented by $N E > E_0 \propto 1/E_0^\gamma$, where γ is 0.5 for energies above 0.8 Bev/nucleon. N is the number of nuclei with an energy greater than E_0 per nucleon. The flux measured at $\lambda = 30^\circ$ N gives an exponent $\gamma = 0.5$. At energies below about 0.75 Bev/nucleon the spectrum seems to get steeper. The flux of heavy nuclei measured on two night flights shows no significant difference from the day flux. Solar activity resulting in flares of importance 1 and 2 shows no measurable correlation with flux of heavy nuclei.

I. INTRODUCTION

SINCE heavy nuclei were first observed in 1948 as part of the primary cosmic radiation,¹ numerous high altitude balloon flights have been made both at Minnesota and off the coast of Cuba in order to study these nuclei in photographic emulsions. Methods previously described²⁻⁶ have been used to determine the charges and energies of the nuclei. The variation of the flux with altitude and zenith angle has been obtained at Cuba (geomagnetic latitude, $\lambda = 30^\circ$ N) and at Minnesota ($\lambda = 55^\circ$ N). A possible diurnal effect has been investigated with two night flights. A possible solar effect has been looked for during two solar flares. The charge spectrum of nuclei of charge ≥ 10 has been determined. The energy spectrum of the $Z \geq 10$ component has been obtained by three methods. The cross section for collision has been measured in glass, emulsion, and air.

II. DAYTIME FLUX OF $Z \geq 10$ AT $\lambda = 55^\circ$ N

If one intends to look for any diurnal or solar variation in the primary cosmic-ray flux, it is necessary first to determine what variations, if any, are introduced by the detector used. Since heavy nuclei are rapidly absorbed by the air of the atmosphere, it is especially important to know accurately the residual air pressure above the detector, and also to know how variations in air pressure change the flux. We have determined the magnitude and angular distribution of the flux of nuclei with charges ≥ 10 on seven different day flights at Minnesota. The flights were all made with "Skyhook" balloons which leveled off at altitudes between 84,000 and 104,000 feet.

The following are the methods that have been used to measure pressure on the various flights. In the early days of flying "Skyhook" balloons, pressure was determined by using theodolite bearings to measure the altitude of the balloon; the residual pressure was then computed assuming a standard atmosphere.⁷ Later, pressure was also measured with mercury manometers and with bellows. Photographing, recording on smoked drums, and telemetering have been used as recording methods. Late in 1950 pressure was successfully measured by a very accurate bellows which acts as a condenser in a crystal oscillator circuit. On October 4, 1950, on a flight which reached 9 g/cm², the bellows and telemetering system were compared with a photographed Wallace-Tiernan gauge. The Wallace-Tiernan gauge is a highly accurate instrument readable to 0.1 g/cm². The two methods gave results which agreed to within 3 percent at pressures of 10 g/cm². General Mills has now adopted this telemetering method of pressure measurement for each flight.

On six of the thirteen flights reported here, there was only one record of the pressure. On six other flights the pressure measured in two different ways agreed within 10 percent. On only one flight did the two pressure records differ by as much as 20 percent. On all but three flights the balloon remained at a constant altitude within the error of pressure measurement. For these three flights an estimate of an average pressure had to be made.

A measurement of the flux of nuclei with $Z \geq 10$ at $\lambda = 55^\circ$ N involves one major difficulty. Slow nuclei of the carbon, nitrogen, oxygen (C,N,O) group can ionize as heavily as fast nuclei of $Z \geq 10$. The only certain way to rule out a nucleus being a slow C,N,O is to follow it through sufficient glass and emulsion so that both the value and rate of change of its ionization density are known. However, this becomes a very time-consuming operation when one is obtaining flux values based on thousands of nuclei. We have corrected for this effect in the following manner.

* This work was supported by the joint program of the ONR and AEC.

¹ Freier, Lofgren, Ney, Oppenheimer, Bradt, and Peters, *Phys. Rev.* **74**, 213 (1948).

² Freier, Lofgren, Ney, and Oppenheimer, *Phys. Rev.* **74**, 1818 (1948).

³ H. Bradt and B. Peters, *Phys. Rev.* **74**, 1828 (1948).

⁴ H. Bradt and B. Peters, *Phys. Rev.* **77**, 54 (1950).

⁵ A. D. Dainton and D. W. Kent, *Phil. Mag.* **41**, 963 (1950).

⁶ Hoang Tchang-Fong, *Ann. phys.* **5**, 537 (1950).

⁷ B. Rossi, *Revs. Modern Phys.* **20**, 537 (1948).

When the plate is scanned for nuclei of $Z \geq 10$, the minimum δ -ray count accepted is set at 1.3 times the minimum count for $Z=10$. From a complete study of 200 heavy nuclei at Minnesota, we know the charge spectrum and the energy spectrum. With this information we can compute what percentage of slow C,N,O we still include in our survey and what percentage of $Z \geq 10$ we exclude by this criterion for track selection. These two corrections are found to be of the same order of magnitude (~ 10 percent) and tend to cancel each other except at the depth where the nuclei of the C,N,O component with energies just above the geomagnetic cutoff reach the end of their range. With a cut-off energy of 0.35 Bev/nucleon this region is from 20 to 25 g/cm². Although we have not followed each nucleus in this critical region in order to eliminate the $Z < 10$ nuclei, the measured flux values do not show any discontinuity in this region. Furthermore, as a direct check on the validity of this correction factor, we found that on completely studying 200 nuclei which had satisfied the criterion necessary for inclusion in the flux of $Z \geq 10$ and which had traversed 15–25 g/cm² before entering the emulsion, 35 of the 200 had charges < 10 . So even in the critical region the number of C,N,O included in the $Z \geq 10$ is about 15 percent, and this is partly compensated for by the exclusion of some fast $Z = 10$ and 11.

On seven different day flights at Minnesota we have measured the angular distribution of the flux of nuclei of $Z \geq 10$. Both C.2 and G.5 Ilford emulsions have been used. The plates have been flown vertically in carefully aligned stacks. 2" \times 4" plates were used on three flights. On all other flights 4" \times 10" plates were flown. The plate stacks were wrapped in black paper and tape, and padded with foam rubber. We have neglected this wrapping and also the 0.05" aluminum of the spherical gondola in which the plates were flown when we have studied the variation of flux with depth in atmosphere. This would amount to a 1–2 g/cm² correction depending on the angle at which the nucleus enters the stack. However, at residual pressures of less than 10 g/cm² this correction should certainly not be neglected.

In order to obtain the angular distribution of the flux of heavy nuclei, the two outside plates in the stack are systematically scanned for all nuclei with δ -ray counts ≥ 1.3 times the δ -day count of a Z of 10 at minimum. The δ -ray count for $Z=10$ is computed from that of carbon which we measure in the plates. On our systematic survey of the plates we count δ -rays on all tracks of more than 1 mm length in the C,N,O group. These nuclei are then followed in other plates and δ -rays counted there. If these nuclei prove to be fast, as shown by their constant ionization over a long range, we use them as calibrating nuclei. We then have the δ -ray counts for fast nuclei in the C,N,O group, and we can determine the δ -ray count for carbon at minimum to within about 10 percent. This error is mostly statistical, and it is sufficiently large to cover any non-uniformity in the development of the plates.

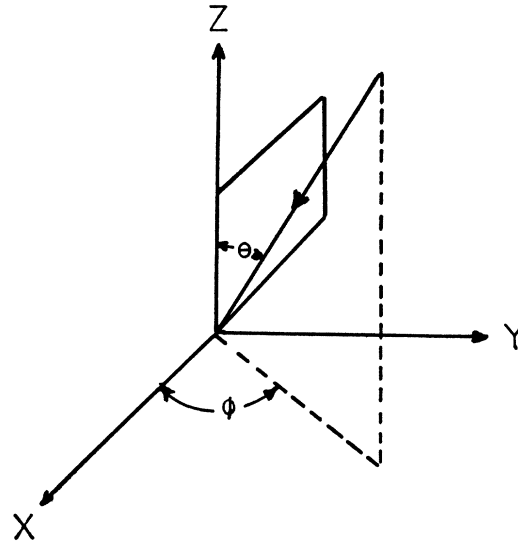


FIG. 1. Definitions of zenith and azimuthal angles in a vertical plate.

The zenith and azimuth angles are measured for each nucleus coming into the stack. The plate on one side of the stack is used for one 180° sector of azimuth, the plate on the other side for the opposite sector. On one flight we checked the equivalence of horizontal and vertical plates as detectors of heavy nuclei. More than 2000 nuclei of $Z \geq 10$ were found on four vertical plates and two horizontal plates. The flux measured in the vertical plate agreed with the flux measured in the horizontal plate within the statistical errors except for zenith angles less than 20° where the horizontal plate proved a poor detector. Nuclei with small zenith angles have short projected lengths in a horizontal plate. We found that we had to decrease our scanning speed in order to obtain 100 percent efficiency in the horizontal plates.

Figure 1 shows the zenith and azimuth angles measured for each nucleus. For particles with angles θ and φ , the effective area presented to the particle is

$$A_{\text{eff}} = A \sin \theta \sin \varphi. \quad (1)$$

This azimuthal sine dependence has been verified for 787 nuclei found on the October 13, 1948, flight. This means that if the nuclei are coming in with azimuthal symmetry, the efficiency of detection is the same in all directions. Since it would take an unlikely coincidence of asymmetry with just the right variation in detection efficiency to give a sine distribution, we conclude that the nuclei are detected with 100 percent efficiency in all directions.

The flux of particles is then given by

$$I = \frac{N}{tA \int_{\varphi_1}^{\varphi_2} \int_{\theta_1}^{\theta_2} \sin^2 \theta \sin \varphi d\theta d\varphi}, \quad (2)$$

TABLE I. Flight data for day flights at $\lambda=55^\circ$ N.

Symbol used on graph	Date of flight	Time at altitude CST	Ceiling pressure (g/cm ²)	Type of pressure measurement*	Total No. of nuclei
Semicircle (diam. below)	7/16/48	1000-1400	24	<i>T</i>	50
Triangle (apex up)	10/13/48	1030-1430	14	<i>T</i>	787
Square	5/24/49	0830-1300	17	<i>T</i>	153
Triangle (apex down)	9/27/49	0800-1530	18	<i>T, Hg_t</i>	207
Circle	2/9/50	1030-1330	18	<i>B, Hg_t</i>	308
Semicircle (diam. at top)	3/29/50	0830-1530	10.5	<i>T, B_t</i>	611
Cross	10/4/50	1015-1545	9	<i>W, B_t</i>	427

* *T* = theodolite; *Hg* = mercury manometer; *B* = bellows; *W* = Wallace-Tiernan gauge; subscript *t* indicates data was telemetered.

where N is the number of nuclei, t the time in seconds, A the area of the emulsion in cm², and I the flux in particles/cm² sec sterad. The zenith angle distribution of flux summed over azimuth has been measured for seven different daytime flights at Minnesota. In Table I the pertinent data for the flights are tabulated. In order to compare fluxes on flights which reach different altitudes, we have plotted in Fig. 2 the fluxes against the residual pressure at ceiling divided by the cosine of the zenith angle, so that the abscissa is proportional to the amount of air the nuclei have traversed. The errors shown are statistical errors ($100/N^{1/2}$ has been used as the percentage error for N nuclei). Pressure errors have been omitted on the graph, but they are about 10 percent on all the flights except on the October 4, 1950, flight where pressure was measured to 3 percent.

III. DAYTIME FLUX OF $Z \geq 10$ AT $\lambda = 30^\circ$ N

Two flights have been made off the coast of Cuba at a geomagnetic latitude of 30° N. The angular distribution of the flux of $Z \geq 10$ has been found in the same manner as at $\lambda = 55^\circ$ N with one important difference. At $\lambda = 30^\circ$ N the vertical magnetic cut-off energy is 3.5 Bev/nucleon for heavy nuclei so that all particles ob-

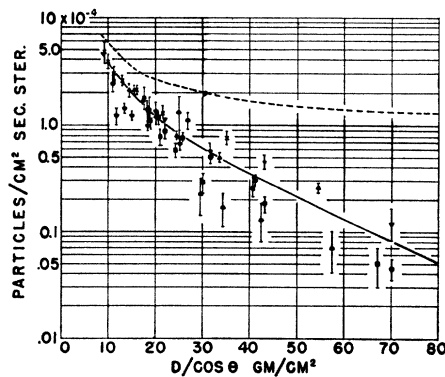


FIG. 2. Daytime flux of $Z \geq 10$ at $\lambda = 55^\circ$ N as a function of depth in atmosphere. The dashed line gives the flux corrected for collision loss in the air. A mean free path of 25 g/cm² was used.

served near the top of the atmosphere are at minimum ionization. This eliminates the difficulty of having to distinguish between a slow nucleus of the C,N,O group and a fast $Z \geq 10$. The emulsions are again calibrated by using long tracks of the C,N,O group and the δ -ray count for $Z = 10$ is computed from the measured value for carbon at minimum.

The data for the two flights are given in Table II. In Fig. 3 we have plotted the flux of $Z \geq 10$ against the residual air pressure at ceiling divided by the cosine of the zenith angle.

Although the earth's magnetic cutoff differs considerably from the west and the east at $\lambda = 30^\circ$,⁸ the flux of particles incident at the top of the atmosphere will be practically independent of zenith angle if the flux is integrated over all azimuths.

If the flux integrated over all azimuths is isotropic with respect to zenith angle at the top of the atmosphere, then the flux at zenith angle, θ , and at a depth, d , in the atmosphere can be given in terms of I_0 , the flux at the top of the atmosphere, by

$$I = I_0 \exp(-d/L \cos \theta), \quad (3)$$

where L is the mean free path for nuclear collisions in

TABLE II. Flight data for day flights at $\lambda = 55^\circ$ N.

Symbol used on graph	Date of flight	Time at altitude CST	Ceiling pressure (g/cm ²)	Type of pressure measurement	Total No. of nuclei
Circle	2/3/49	0900-1530	17.5	<i>Hg, B_t</i>	183
Triangle	11/17/49	0800-1345	20	<i>B_t</i>	228

air. Since the cut-off energies are so high, nuclei are not stopped by ionization, and only the collision loss need be accounted for in Eq. (3). We have fitted the 14 data points to this expression by the method of least squares, and the straight line obtained in this manner is drawn in Fig. 3. The values found for the constants are

$$I_0 = (0.85 \pm 0.08) \times 10^{-4} Z \geq 10 \text{ nuclei/cm}^2 \text{ sec sterad,}$$

$$L = 21 \pm 2 \text{ g/cm}^2.$$

We have also measured the relative numbers of C,N,O nuclei and $Z \geq 10$ nuclei with zenith angles from $0-30^\circ$. The ratio is

$$R = \frac{I_{(0-30^\circ)}(C,N,O)}{I_{(0-30^\circ)}(Z \geq 10)} = 3.9 \pm 0.7$$

and represents the ratio at about 20 g/cm² of air. If we assume that the computed mean free path of 21 ± 2 g/cm² in air is for an average Z of 15, we can compute the corresponding mean free path for Z of 7. These mean free paths are considerably different, which makes R a function of atmospheric depth. Correcting R measured at 20 g/cm² to the top of the atmosphere, we

⁸ M. Vallarta, Phys. Rev. 74, 1837 (1948).

obtain a flux at the top of the atmosphere for C,N,O of

$$I_0 = 2.7 \pm 0.5 \times 10^{-4} \text{ C,N,O nuclei/cm}^2 \text{ sec sterad.}$$

IV. CHARGE SPECTRUM OF HEAVY NUCLEI

On October 13, 1948, a large stack of sixty-eight $4'' \times 10''$ Ilford C.2 100μ emulsions was flown at Minnesota. These plates were used to study the charge spectrum of the nuclei. Two hundred heavy particles with zenith angles from 0° – 30° were followed through the stack to determine energies, charges and cross section for collision. Seven of these two hundred nuclei stopped in the emulsion and 56 in the glass; 19 were slowing down enough so that energy and charge could be accurately determined from change in ionization.

The charge distribution for these nuclei is shown in Fig. 4. For the 82 nuclei which stopped or slowed down, the charge is accurate to within 10 percent. For particles which merely went through the stack or suffered collisions, the charge can usually be determined within 20 percent. Particles whose charges have been deter-

TABLE III. Relative abundances of heavy nuclei.

Element	Z	Elemental abundance (Brown)	Cosmic-ray abundance at 15 g/cm^2 $\lambda = 55^\circ \text{ N}$
Ne	10	9–240 (uncertain)	8
Mg	12	9	7
Si	14	10	10
S	16	3.5	3
A	18	0.1–2.2	3
V	23	Negligible	5
Fe	26	18	9
Ni	28	1	1
All $Z \geq 10$		54 (using Ne=9)	56
C,N,O		460	260

mined by either means are included in the charge distribution.

The relative numbers of C,N,O and $Z \geq 10$ nuclei were measured for nuclei with zenith angles from 0° – 30° . The ratio at $\lambda = 55^\circ \text{ N}$ and at 15 g/cm^2 residual pressure is

$$R = 4.6 \pm 1.3.$$

In Fig. 4 we have used this ratio in order to plot the C,N,O abundances along with the $Z \geq 10$ abundances. The relative number of the C,N,O nuclei was obtained from only 35 slow particles and is therefore not statistically very significant. Also, with the 10 percent accuracy we obtained in Z determination, it was impossible to completely resolve the peaks in the C,N,O group. The relative abundances of C, N, and O have been studied more extensively by Bradt and Peters.⁴

We can compare the cosmic-ray abundances of heavy nuclei with elemental abundances as summarized by Brown.⁹ For elements with charges ≥ 10 , there are peaks in the abundance curve at neon, magnesium, silicon,

⁹ H. Brown, *Revs. Modern Phys.* **21**, 625 (1949).

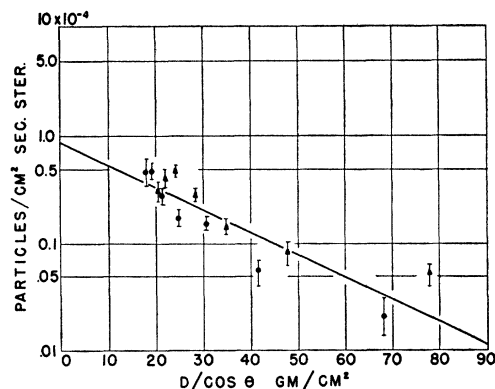


FIG. 3. Flux of $Z \geq 10$ at $\lambda = 30^\circ \text{ N}$ as a function of depth in atmosphere. The straight line is a least mean squares fit to the data.

sulfur, argon, and iron. All of these show up in the heavy nucleus abundances with the addition of a peak at $Z = 23$ (vanadium) which has negligible abundance according to measurements of meteoritic and stellar abundances. Some of these nuclei could be iron whose charge is estimated too low, but it would be difficult to explain them all in this way. Many of them may be nuclei resulting from a collision which only slightly decreases the charge of an iron nucleus. Such collisions have been observed in the emulsion. In Table III are listed the relative elemental abundances for elements with charges ≥ 10 normalized at silicon. For the cosmic-ray abundances the number of nuclei with a given Z was taken to be the measured number of nuclei with that charge, Z , plus one-half of the measured number of nuclei with a charge of $Z \pm 1$.

Only three nuclei of the 200 had charges significantly greater than that of iron. Two of them were slow. Since their great number of δ -rays made counting difficult, they could conceivably be iron nuclei. However, one of them went a great distance in the stack and was definitely heavier than iron. The relative abundance of nickel is high enough that it is not at all surprising to

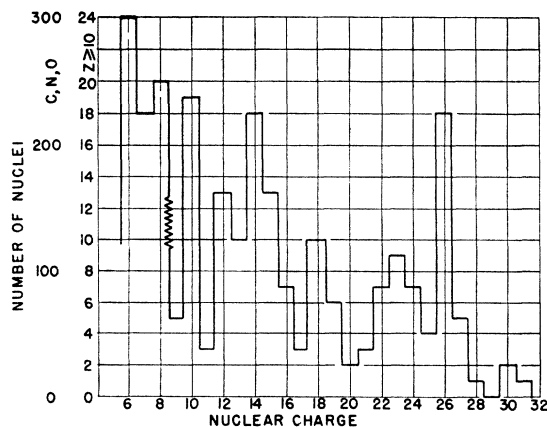


FIG. 4. Charge distribution of heavy nuclei at $\lambda = 55^\circ \text{ N}$. Residual pressure equals 15 g/cm^2 .

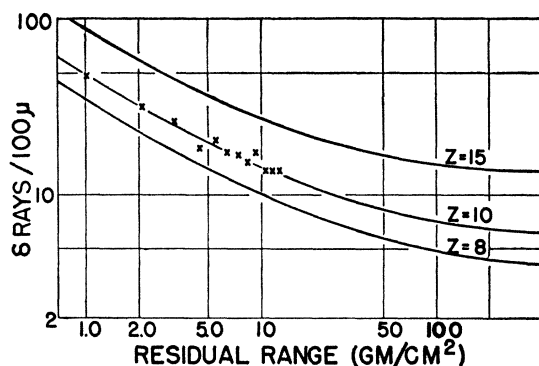


FIG. 5. Experimental and theoretical variation in δ -ray counts with residual range for a nucleus of charge 10 stopping in the emulsion.

see some nuclei with charges greater than that of iron. We have already reported² one nucleus with a charge of 41 ± 4 . It is the heaviest one we have seen and is the only nucleus we have found heavier than nickel.

V. CROSS SECTION FOR NUCLEAR COLLISION

The 200 particles from which we obtained the charge spectrum were also used to determine the cross section for nuclear collisions. The 200 particles were selected for study because (i) their zenith angles were $< 40^\circ$, and (ii) their possible range in the stack of plates was at least 20 g/cm^2 . It was possible for a particle to have as much as 70 g/cm^2 range in the stack of plates. The 200 particles thus chosen were followed through the stack, and their δ -rays were counted. The sudden disappearance of a track between two emulsions or a decrease in its δ -ray count indicated a collision in the glass. We could detect any collision of a heavy nucleus which changed the charge of that nucleus by 10 percent or more.

At Minnesota many particles stop by ionization; therefore, we must be sure that we can differentiate a stopping in the glass from a collision in glass. By studying very carefully the δ -ray counts on the seven nuclei which stopped in the emulsion and whose ranges were, therefore, accurately known, we determine how well the change in δ -ray counts agrees with the theoretically expected variation in ionization with range. Figure 5 shows the agreement between the experimental and theoretical δ -ray counts for a nucleus of charge 10 which stopped in the emulsion. A particle was said to stop in the glass only if its δ -ray count agreed within

TABLE IV. Mean free paths in g/cm^2 of glass.

In-coming charge	$\lambda = 55^\circ \text{ N}$		$\lambda = 55^\circ \text{ N}, E \geq 1 \text{ Bev/nucleon}$		$\lambda = 30^\circ \text{ N}$		L_{geom}
	L_{exp}	No. of collisions	L_{exp}	No. of collisions	L_{exp}	No. of collisions	
6, 7, 8	55 ± 13	17	42 ± 11	13	39 ± 20	2	33
10-20	44 ± 6	46	36 ± 6	38	34 ± 10	12	24
≥ 20	50 ± 10	21	33 ± 8	18	29 ± 12	6	18

the experimental errors with the theoretically expected count for a stopping particle. Otherwise, a particle which disappeared in the glass was said to have suffered a collision.

In Table IV we show the experimental mean free path determined from the 200 particles chosen for study. The errors indicated are statistical errors based on the number of observed collisions. We can compare the measured values with geometric mean free paths. For two nuclei to interact with one another, it is reasonable to expect that they must overlap by a distance equal to the range of nuclear forces. For two nuclei with radii, r_1 and r_2 , the geometric cross section is then

$$\sigma = \pi[r_1 + r_2 - 1.4 \times 10^{-13}]^2. \quad (4)$$

For the radius of a nucleus with mass number, A , we use

$$r = [1.4A^{1/3} \times 10^{-13}] \text{ cm}. \quad (5)$$

The mean free path is then obtained from this geometric cross section by

$$L = \rho / \sum_i n_i \sigma_i. \quad (6)$$

L is the mean free path in g/cm^2 , ρ is the density of material in g/cm^3 , n_i is the number of atoms/ cm^3 , and σ_i is the cross section in cm^2 for each component of the material. Considering glass as SiO_2 and using the measured density of 2.44 g/cm^3 , we obtain the geometric mean free paths which are shown in the last column of Table IV.

The mean free paths determined experimentally at Minnesota are much longer than the geometric mean free paths. This is in disagreement with the result of Bradt and Peters,⁴ who found at $\lambda = 30^\circ \text{ N}$ values consistent with the geometric cross section. In an effort to determine the reason for this discrepancy, we eliminated from our measurement of path length at Minnesota all the nuclei which were slow. This allows a measurement of the mean free path for those nuclei whose energies are greater than about 1 Bev/nucleon. The result for the group of faster particles is much closer to the geometric value, but still significantly greater than the geometric mean free path. We determined the mean free path at $\lambda = 30^\circ \text{ N}$ where the average energy of the particles is still higher and found values about the same as for energetic Minnesota particles. The results are shown in Table IV.

The mean free path for collision has also been measured in emulsion. Here we do not have the problem of missing a collision since the actual collision can be seen. A total of 43 collisions of $Z \geq 10$ has been observed in the emulsion. Some of the collisions were observed while following particles through the stack; the rest while scanning plates to obtain flux measurements. The results obtained by the two methods agree; combined they give

$$L_{\text{emulsion}} = 47 \pm 7 \text{ g/cm}^2.$$

The geometric mean free path in emulsion can be

computed using the emulsion composition given by Ilford. For an incoming charge of 16 the geometric mean free path in emulsion is

$$L_{\text{emulsion}}(\text{geom}) = 36 \text{ g/cm}^2 \quad (Z = 16).$$

We have one other mean free path determination. That is the value for air deduced from the angular distribution at Cuba (Sec. III),

$$L_{\text{air}} = 21 \pm 2 \text{ g/cm}^2.$$

The mean free path corresponding to a geometric cross section for air with an incoming $Z = 16$ is

$$L_{\text{air}}(\text{geom}) = 18.5 \text{ g/cm}^2 \quad (Z = 16).$$

In order to compare the mean free paths measured in such different ways we must investigate the essential differences in the measurements. The glass measurements include all collisions which change the charge of the heavy nucleus by 10 percent or more. The incoming

TABLE V. Frequency of various types of collisions in glass.

Incoming Z	$Z \geq 10$ goes on (%)	$Z = 3-8$ goes on (%)	Only alphas and protons go on (%)	Total number of collisions
20-26	50	25	25	30
10-19	25	25	50	57
6-8		25	75	16

charge can be identified so that the division into the Z groups can be made. The collisions can be classified into two groups.¹⁰ The heavy nucleus may go on in the same direction with its charge reduced. An example of this type of collision is shown in Fig. 6. In the second type of collision, nothing heavier than an alpha-particle penetrates. Figure 7 shows a collision of this type. Table V gives the relative frequency of these types of collision in glass.

The emulsion mean free path measurement differs from the glass measurement in several ways. In the



FIG. 6. A collision in which an incoming nucleus of charge 16 breaks up into three penetrating particles of charge 7, 4, and 2 which go forward in the same direction.

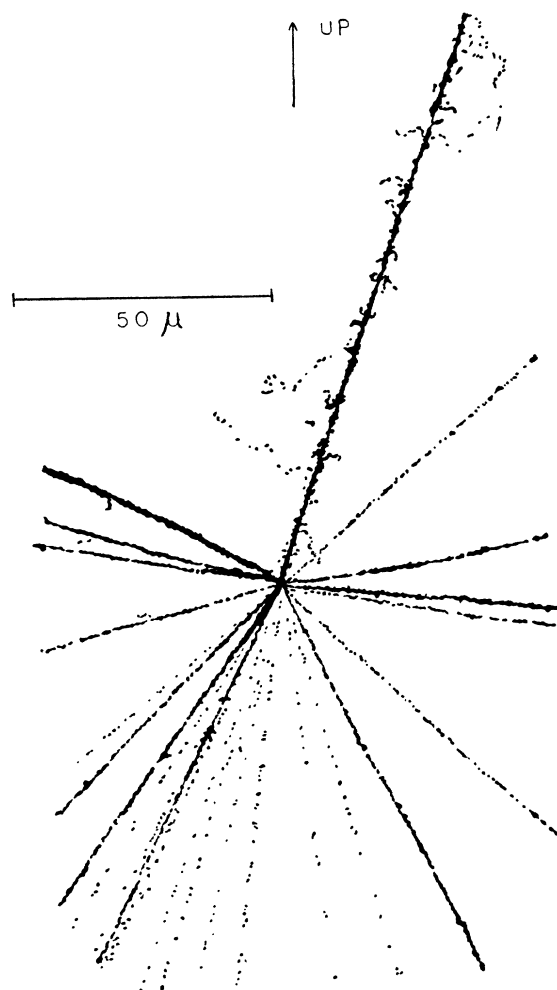


FIG. 7. A collision which results in the complete break-up of the incoming heavy nucleus whose charge was about 15.

¹⁰ H. Bradt and B. Peters, Phys. Rev. **75**, 1779 (1949).

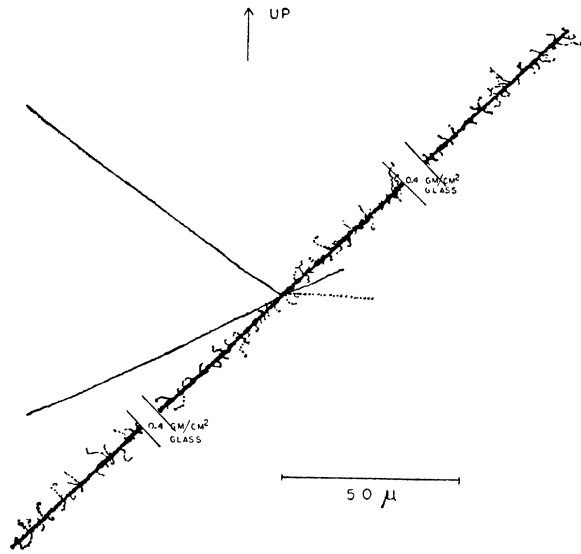


FIG. 8. A collision in which the incoming nucleus of charge 14 goes on unchanged in charge or direction. Three protons of energies 1.0, 9.2, and 10.2 Mev end in the emulsion. The other particle is probably a proton of about 130 Mev.

first place no collisions are missed in the emulsion. Twelve percent of the 64 collisions which we have now observed in the emulsion involve no detectable change either in the charge or the direction of the heavy primary. Figure 8 shows an example of such a collision in which four low energy protons seem to be evaporated from the target with no noticeable change in the heavy primary. Three of the eight cases we have found involve the evaporation of only one particle from the target nucleus. Such collisions would not be detected if they occurred in the glass. Collisions of this type have been observed before.^{4,6} Tchang-Fong has considered and rejected the possibility that such events are the result of electromagnetic rather than nuclear excitation.

We have not been able to identify the charge for every nucleus whose path is included in the emulsion path length measurement. The path length was obtained from all nuclei whose charges were ≥ 10 . From the measured charge distribution we can calculate that the average cross section for the $Z \geq 10$ group is that of $Z=16$. This would vary with atmospheric depth, but with an integral energy spectrum with an exponent of 0.8 (see Sec. VI) and with geometric cross sections in air, the average cross section would change only 10

TABLE VI. Ratio of experimental to geometric cross section.

In-coming charge	$\lambda = 55^\circ \text{ N}$ all energies	Glass		Emulsion $\lambda = 55^\circ \text{ N}$	Air $\lambda = 30^\circ \text{ N}$
		$\lambda = 55^\circ \text{ N}$ $E \geq 1$ Bev/nucleon	$\lambda = 30^\circ \text{ N}$		
6-8	0.60 ± 0.15	0.80 ± 0.20	0.8 ± 0.4		
10-20	0.55 ± 0.08	0.67 ± 0.11	0.7 ± 0.2		
10-26				0.77 ± 0.15	0.88 ± 0.09
≥ 20	0.36 ± 0.07	0.55 ± 0.13	0.6 ± 0.2		

percent from the top of the atmosphere down to 50 g/cm² of residual pressure. Therefore the assumption of an average cross section equal to the cross section of $Z=16$ is valid within the accuracy of our measurements. We have used the geometric cross section for an incoming nucleus of $Z=16$ to compare with the measured cross sections in air and emulsions for all nuclei of $Z \geq 10$. Table VI gives a summary of the experimental results in terms of the ratio of the experimentally determined cross sections to the geometric cross section.

The cross sections are significantly smaller than geometric except for the air value found from the angular distribution at $\lambda=30^\circ \text{ N}$. In Table V we saw that at least 25 percent of the collisions in glass of the $Z \geq 10$ component resulted in a nucleus whose charge was ≥ 10 penetrating further. Thus we should reasonably expect the ratio of experimental to geometric cross sections for air to be about 25 percent smaller than for glass. We do not understand why the observed ratio of experimental to geometric cross sections is, instead, even higher than that for glass. Since the ratio in air was determined by an indirect method, we place more weight on the glass and emulsion values. From those it seems that the cross section for the collision of two nuclei at energies greater than 1 Bev/nucleon is about three-fourths the geometric cross section.

VI. THE ENERGY SPECTRUM OF HEAVY NUCLEI

The energy spectrum of the heavy nuclei has been determined in three different ways with fair consistency. We have used the angular distribution, the latitude effect, and the number of stopping particles to give estimates of the exponent in a power representation of the energy spectrum.

Figure 2 shows the manner in which the flux of nuclei with charges ≥ 10 decreases with increasing air path. This decrease in flux is due to loss of particles both by collision and by ionization. If we correct the measured flux for collision loss in the atmosphere, we obtain the flux at the top of the atmosphere of these particles which have enough energy to penetrate down to our detector. We have corrected the measured flux using a collision mean free path of 25 g/cm²; the resulting flux at the top of the atmosphere is given by the dashed curve in Fig. 2. This assumed mean free path corresponds to 0.75 of the geometric cross section in air for a nucleus of charge 16. Since the relative charge distribution is a function of atmospheric depth, the choice of $Z=16$ as an average charge for all depths is only an approximation, but the error is less than 10 percent.

The dashed curve in Fig. 2 then gives us the flux at the top of the atmosphere of nuclei with energies great enough to penetrate to the detector as a function of the atmospheric depth. We have obtained from this flux an integral energy spectrum by plotting the flux against the energy necessary for a nucleus of charge=16 to penetrate the required amount of air. The results are shown in Fig. 9. We have included a point at 3.8

Bev/nucleon corresponding to the vertical flux at $\lambda=30^\circ$ N.

We shall assume that the integral energy spectrum is of the form

$$NE > E_0 \propto 1/E_0^\gamma, \quad (7)$$

where N is the number of particles with energies greater than E_0 . Figure 9 shows a sharp break in the energy spectrum at about 0.7 Bev/nucleon. The value of γ changes from 1.7 for low energies to 0.5 for energies above 0.8 Bev/nucleon.

If we assume that the integral energy spectrum with the 0.5 exponent extends to higher energies, we see that the vertical flux measured at 30° N latitude falls on this line (see Fig. 9). The penumbra region between the main cone and the shadow cone is fairly wide at $\lambda=30^\circ$ ⁸ so we have used the average energy with an error equal to the half-width of the penumbra region. If, in the conventional manner,^{11,12} we use the vertical flux measured at $\lambda=55^\circ$ (cut-off energy=0.35 Bev/nucleon) and at $\lambda=30^\circ$ (cut-off energy= 3.8 ± 0.5 Bev/nucleon), we find for the exponent in the integral power spectrum

$$\gamma = 0.87 \pm 0.13.$$

This value, however, merely represents an average γ between the energies 0.35 and 3.8 Bev/nucleon.

A completely independent check on the form of the energy spectrum can be obtained from the 200 heavy nuclei studied on the October 13, 1948, flight. Eighty-two of these nuclei either stopped in the stack or were slow enough to allow an accurate determination of the energy. A lower limit can be set on the energies of the other nuclei. Considering the criteria which had to be satisfied by a particle before it was included in this survey, we could compute the energy range for which the stack is an efficient detector. This energy range is a function of the charge of the particle. In Fig. 10 we have plotted the integral energy spectrum obtained from three groups of nuclei. There is good agreement with the results obtained from the angular distribution and latitude effect. The $Z=9-12$ group which measures the spectrum in the range from 0.45 to 0.8 Bev/nucleon shows an exponent of 0.85 significantly higher than the value of 0.5 obtained from the other two charge groups in the region from 0.6 to 1.6 Bev/nucleon.

The energy spectrum of heavy nuclei can be compared with the spectrum of protons obtained by Winckler, *et al.*¹² They obtained an exponent of 0.9 from 1 to 14 Bev with some evidence that the spectrum becomes flatter below 1 Bev. However, except for the measurement of Pomerantz at 69° N,¹³ there is not much data below 1 Bev, and the form of the proton energy spectrum is certainly not well known in this region. The evaluation of the energy spectrum of the heavy nuclei from the angular distribution is subject

¹¹ M. Vallarta, *Phys. Rev.* **77**, 419 (1950).

¹² Winckler, Stix, Dwight, and Sabin, *Phys. Rev.* **79**, 656 (1950).

¹³ M. Pomerantz, *Phys. Rev.* **77**, 830 (1950).

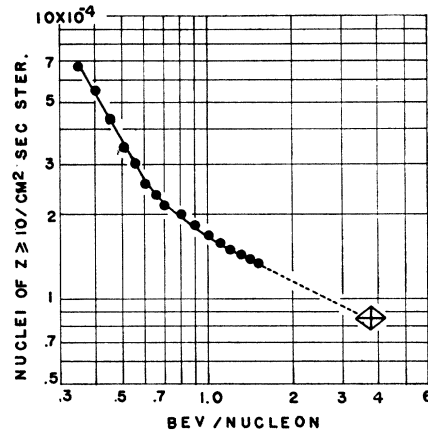


FIG. 9. An integral energy spectrum of nuclei with charges ≥ 10 . The circled data were obtained from an atmospheric absorption measurement at $\lambda=55^\circ$ N. The point at 3.8 Bev/nucleon represents the vertical flux at $\lambda=30^\circ$ N.

to many uncertainties. If the cross section for collision becomes smaller at low energies, as is indicated by our measurements (Table IV), the energy spectrum obtained from the atmospheric absorption would flatten out some at low energies. However, there would still be a steeper form of the spectrum at low energies than at energies above about 0.8 Bev/nucleon. The energy spectrum in this region from 0.35 to 0.80 Bev/nucleon can be investigated more accurately by studying the differential energy spectrum of the C,N,O component.¹⁴

VII. DIURNAL VARIATION IN FLUX

We have studied the flux of nuclei with charges ≥ 10 on two different night flights. The angular distribution was determined in the same manner as for all other flights. Table VII gives the flight data, and Fig. 11 gives the flux measured on these two flights.

The first night flight we made led us to believe that the flux at night might be low.¹⁵ However, the residual pressure on this flight varied from 23 to 35 g/cm², being as high as 30 g/cm² for 10 percent of the flight time. The

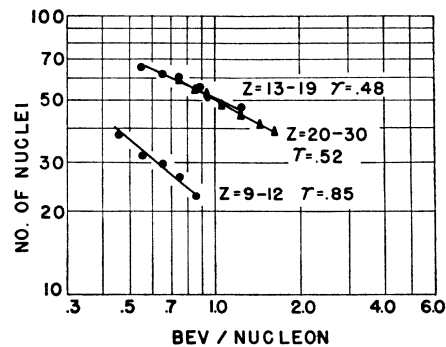


FIG. 10. An integral energy spectrum of nuclei with charges ≥ 10 obtained from the energy determination of 200 nuclei at $\lambda=55^\circ$ N.

¹⁴ Reynolds, Ritson, and Woodruff, *Phys. Rev.* **83**, 197 (1951).

¹⁵ Freier, Ney, Naugle, and Anderson, *Phys. Rev.* **79**, 206 (1950).

TABLE VII. Flight data for night flights and solar flare flights.

Symbol used on graph	Date of flight	Time at altitude CST	Ceiling pressure (g/cm ²)	Type of pressure measurement	Total No. of nuclei
Circle— Fig. 11	10/26/49 to 10/27/49	1630 0700	25	B, Hg	529
Triangle— Fig. 11	4/13/50 to 4/14/50	1830 0700	14	B	803
Circle Fig. 13	2/15/50 to 1900	1800	18	B	50
Diamond— Fig. 13	9/2/50	1530 to 1800	12–16	B _t , B	236

average of 25 g/cm² is simply a time average of the altitude. A more satisfactory night flight on which the pressure was maintained at 14 g/cm² was made in April, 1950. The flux of heavy nuclei on this flight agrees very well with the daytime flux values. Since this second flight had a much more reliable pressure record, we give this result more weight. Lord and Schein^{16,17} have recently reported a night flux 2.5 times smaller than the day flux at 15 g/cm² residual pressure. In view of these conflicting results and the importance of the problem to theories of cosmic-ray origin, the diurnal variation of the flux of heavy nuclei could bear more detailed investigation.

On the October 26, 1949, night flight the star density in the emulsions was measured and compared to the density measured during the day.¹⁸ No appreciable difference was obtained in the star densities. This is in agreement with Lord and Schein.¹⁶

VIII. AZIMUTHAL ASYMMETRY

A recording compass was flown on both of the night flights, but failed both times to record for the whole flight time. The record showed that the October 26

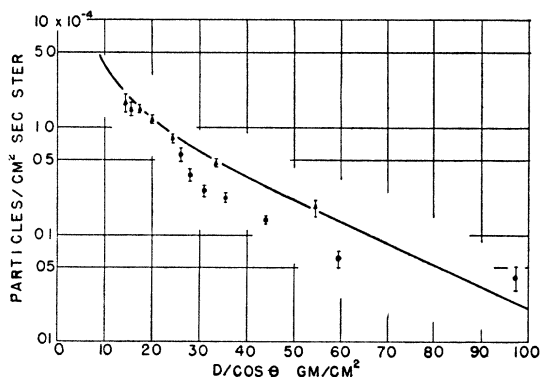


FIG. 11. Night-time flux of $Z \geq 10$ at $\lambda = 55^\circ$ N as a function of depth in atmosphere. The curve gives the daytime flux at $\lambda = 55^\circ$ N.

¹⁶ J. Lord and M. Schein, *Phys. Rev.* **78**, 484 (1950).

¹⁷ J. Lord and M. Schein, *Phys. Rev.* **80**, 304 (1950).

¹⁸ G. Anderson and J. Naugle, M.S. theses (University of Minnesota, 1950).

flight was fortuitously oriented about 25 percent of the time with no record of the orientation for 50 percent of the flight time. On the April 13 night flight an attempt was made to orient the plates. For 25 percent of the flight the recorder showed constant orientation of the plates within $\pm 10^\circ$. For the remainder of the flight the recorder did not function, and the orientation is unknown during this time.

On both of these night flights an azimuthal asymmetry was observed. On October 26 the flux as a function of azimuth varied roughly sinusoidally about the mean with an amplitude of about 50 percent of the mean and with the minimum near the east. On April 13 the asymmetry was only about 10 percent with a minimum 70° N of E. The presence of such an asymmetry at night is certainly not well-founded; however, the agreement, though rough, seems to be more than chance. An experiment is in progress to investigate this problem.

TABLE VIII. Solar activity during flight times.

Date	Number of flares reported during flight	Number of flares reported during 8 hours preceding flight	Activity ^a
7/16/48	0	0	Quiet
10/13/48	0	4	Active
2/3/49	1	7	Active ⁺
5/24/49	1	0	Active ⁻
9/27/49	0	3	Active
10/26, 27/49	0	0	Quiet
11/17/49	0	4	Active
2/9/50	0	0	Quiet
2/15/50	b	b	b
3/29/50	0	1	Active ⁻
4/13, 14/50	0	8 (very small)	Active
8/2/50	2	5	Active ⁺
10/4/50	0	0	Quiet

^a The flights have been classified in four groups: quiet, no flares; active⁻, 1–2 flares; active, 3–4 flares; active⁺, more than 5 flares.

^b Observation of flares was intermittent because of clouds. Period of February 12–February 20 was one of great activity on the sun with 7 flares being observed on February 16. Activity probably went unobserved on February 15.

The daytime azimuthal effect has been checked carefully with a stack flown at altitude for 190 minutes.¹⁹ For 140 minutes the plates were held with constant orientation within $\pm 15^\circ$ and to within $\pm 35^\circ$ for 184 of the 190 minutes. The direction of incidence of each nucleus was determined. The number of nuclei in each of the four quadrants of azimuth is shown in Fig. 12. The results show no asymmetry. The poor statistics do not exclude there being an asymmetry as great as 15 percent.

IX. EFFECT OF SOLAR ACTIVITY ON HEAVY FLUX

Many people have reported increased cosmic-ray activity during the now well known solar flare of November 19, 1949.^{20–23} In an attempt to discover

¹⁹ Ney, Linsley, and Freier, *Phys. Rev.* **79**, 206 (1950).

²⁰ Doubillier, *Compt. rend.* **229**, 1096 (1949).

²¹ D. C. Rose, *Phys. Rev.* **78**, 181 (1950).

²² Forbush, Stinchcomb, and Schein, *Phys. Rev.* **79**, 501 (1950).

²³ J. Clay and H. F. Jongen, *Phys. Rev.* **79**, 908 (1950).

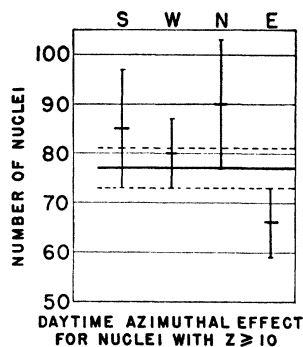


FIG. 12. The daytime azimuthal effect measured on February 9, 1950. The solid line gives the number of nuclei averaged over the four quadrants of azimuth.

whether solar activity affected the flux of heavy nuclei, we have flown two balloons after learning of the outbreak of unusual activity on the sun. The flight data is given in Table VII. The flux measured on these two flights is shown in Fig. 13.

These flights have not measured the flux of heavy nuclei very accurately because of the short duration of the flights and the poor altitude records. On one of the flights the balloon was above 80,000 feet for only one hour, and not at a constant altitude for even that hour. On the flight of August 2, the pressure records disagreed, and the two extremes of pressure have been indicated on the graph. We estimate the pressure errors on these two flights to be of the order of 20 percent. We include these flux measurements, however, because they give some limits, at least, on the magnitude of any solar effect.

In Table VIII we have listed the solar activity for each of the days on which we have measured the flux. These data were kindly furnished by A. H. Shapley of the National Bureau of Standards. The flares tabulated here were all of magnitude 1 and 2 except for the 8 very small flares reported on April 13, 14, 1950, the time of the second night flight. February 3, 1949, the day of one of the flights at $\lambda=30^\circ$ N, was as active as either

February 15, 1950, and August 2, 1950, when we tried to measure the effect of the sun's activity.

It appears that the usual solar activity resulting in flares of importance 1 and 2 affects the flux of heavy nuclei to only a small degree, if at all. The activity of November 19, 1949, was much more outstanding, with the flare being rated importance 3 and lasting significantly longer than the flares occurring on the days we have measured the flux

The authors wish to express their sincere thanks to the many people who have contributed to this study, but especially to A. H. Shapley, who so kindly furnished

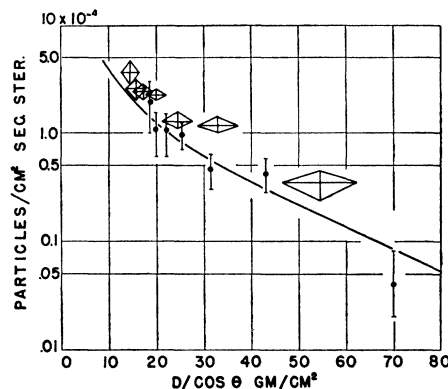


FIG. 13. Flux of $Z \geq 10$ at $\lambda=55^\circ$ N as a function of depth in atmosphere during two times of increased solar activity. The solid line gives the flux during times of more normal solar activity.

the solar activity data, to John Linsley, who built the orienters used on two of the flights, and to Duwayne Thon and David Church, who have helped with so many of the details of the flights. Charles Moore and William Huch of the General Mills Aeronautical Research Laboratories have been very helpful and cooperative in arranging the flights. We appreciate the cooperation and support of the Office of Naval Research.